

<https://doi.org/10.1038/s41525-025-00499-z>

# Exploring gene-phenotype relationships in *GRIN*-related neurodevelopmental disorders



Jong Ho Cha<sup>1</sup>, Jee Min Kim<sup>1</sup>, Hee-Jeong Yun<sup>1</sup>, Hyungjin Chin<sup>1</sup>, Hye Jin Kim<sup>1</sup>, Woojoong Kim<sup>1</sup>, Soo Yeon Kim<sup>1,2</sup>, Byung Chan Lim<sup>1</sup>, Ki Joong Kim<sup>1</sup>, Seungbok Lee<sup>1,2</sup>✉ & Jong-Hee Chae<sup>1,2</sup>

The *GRIN* family is implicated in neurological disorders, such as global developmental delay (GDD) and epilepsy. We reviewed 31 patients with *GRIN*-related neurodevelopmental disorders at Seoul National University Hospital; all exhibited profound GDD, with 58.1% unable to walk independently and 74.2% unable to speak meaningful words. In a pooled analysis with the *GRIN* portal data (<https://grin-portal.broadinstitute.org/>), patients with missense or in-frame variants had significantly higher rates of profound GDD (74.3% vs. 30.4%,  $p < 0.001$ ) and movement disorders (69.0% vs. 41.4%,  $p < 0.01$ ) than those with protein-truncating variants. Furthermore, missense or in-frame variants in the M3 and M4 helices of the transmembrane domain were significantly associated with profound GDD (M3 helix: adjusted odds ratio [aOR] 8.48; 95% confidence interval [CI] 2.79–25.76; M4 helix: aOR 3.14; 95% CI 1.39–7.09) compared to those in other domains. Our findings highlight the importance of detailed variant characterization to inform personalized treatment strategies.

The N-methyl-D-aspartate (NMDA) receptor, a ligand-gated ion channel, regulates excitatory neurotransmission and contributes to higher cortical functions, such as learning and memory, by coordinating neuronal network activity within the synapse<sup>1,2</sup>. The *GRIN* gene family encodes two glycine-binding GluN1 subunits (*GRIN1*) and two glutamate-binding GluN2/3 subunits (*GRIN2A*, *GRIN2B*, *GRIN2C*, *GRIN2D*, and *GRIN3*) of the NMDA receptor. Among the *GRIN* genes, four are currently listed in the Online Mendelian Inheritance in Man (OMIM) database as causative genes for *GRIN*-related neurodevelopmental disorders (NDDs): *GRIN1* (OMIM #614254), *GRIN2A* (OMIM #616139), *GRIN2B* (OMIM #613970), and *GRIN2D* (OMIM #617162)<sup>1,3,4</sup>. All disorders associated with these four genes follow an autosomal dominant inheritance pattern. The distribution of variant types varies by database, with more than 65% being missense and protein-truncating variants (PTVs) accounting for approximately 20%<sup>5</sup>.

The NMDA receptor subunits exhibit a modular domain architecture comprising amino-terminal domains (ATDs), ligand-binding domains (LBDs), transmembrane domains (TMDs), and intracellular carboxy-terminal domains (CTDs)<sup>6</sup>. The TMD functions as the pore-forming region, consisting of three transmembrane helices (M1, M3, and M4) and a re-entrant loop (M2). Although the molecular structures of the NMDA receptor subunits share common features<sup>3</sup>, each *GRIN* variant presents distinct neurological phenotypes, primarily attributed to differences in expression patterns. *GRIN2B* variants are associated with profound global

developmental delay (GDD) and autism spectrum disorder (ASD), as GluN2B subunits are expressed during early postnatal development. In contrast, *GRIN2A* variants are highly associated with epilepsy, as GluN2A expression increases significantly upon birth<sup>7</sup>.

With advancements in next-generation sequencing (NGS), loci corresponding to specific domains of the NMDA receptor have been identified<sup>8</sup>. Recent findings by Xu et al.<sup>8</sup> showed that the gain-of-function (GoF) variants in the M3 helix of the TMD are associated with neurological disorders, such as epilepsy and GDD. Additionally, the M4 helix plays a critical role in receptor function, including channel opening and transmembrane modulation<sup>1</sup>. Given that each domain encodes a protein with a distinct function, it is possible to infer the relationship between specific domains and phenotypes among the diverse neurological phenotypes of *GRIN*. Accordingly, we aimed to analyze the association between certain *GRIN* domains, particularly the M3 and M4 helices of the TMD, and neurological phenotypes. The recently developed *GRIN* Portal (<https://grin-portal.broadinstitute.org/>) has facilitated the exploration of genotype–phenotype correlations and the phenotypic features of *GRIN* variants. However, a comprehensive characterization of neurological phenotypes in relation to specific variant subtypes and locations remains limited.

This study was conducted in 31 Korean pediatric patients with pathogenic *GRIN* variants who visited a tertiary center with chief complaints

<sup>1</sup>Department of Pediatrics, Seoul National University College of Medicine, Seoul National University Children's Hospital, Seoul, South Korea. <sup>2</sup>Department of Genomic Medicine, Seoul National University Hospital, Seoul, South Korea. ✉e-mail: [for3guy@naver.com](mailto:for3guy@naver.com)

of GDD or seizures. In this study, we conducted an in-depth description of the neurological phenotypes observed in these patients. Through a pooled analysis of previously reported *GRIN* variants from the GRIN Portal, we investigated the genotype–phenotype correlations in *GRIN*-related NDDs, with a particular focus on the relationship between variant location and the presence or severity of neurological phenotypes.

## Results

### Identification of *GRIN* mutations

We included 31 pediatric patients with 28 distinct *GRIN* variants, including 22 missense variants, one nonsense variant, two in-frame variants, and three large deletions (Table 1). The most prevalent *GRIN* variant was *GRIN2B*, followed by *GRIN1*, *GRIN2A*, and *GRIN2D*. Among these, 22 patients were

confirmed as de novo mutations through trio analysis and were confirmed as pathogenic or likely pathogenic according to the American College of Medical Genetics (ACMG) criteria. One child (Seoul National University Hospital [SNUH] 31) with a *GRIN2D* variant was confirmed to have two discrete de novo missense variants in *cis*: p.Asn830Ser and p.Asn844His. Three recurrent *GRIN2B* variants were identified within the cohort: c.2459G>C (found in SNUH 13 and SNUH 19), c.2539C>T (found in SNUH 15 and SNUH 27), and c.2287G>A (found in SNUH 29 and SNUH 30, who are monozygotic twins).

Among the 25 *GRIN* variants (missense, in-frame, and PTVs) identified, 13 were not previously reported in ClinVar. All three deletions involved *GRIN2B*, with deletion sizes of 6.6 Mb (SNUH 14), 257 kb (SNUH 16), and 4.2 Mb (SNUH 18), respectively. When stratifying the 25 *GRIN* variants

**Table 1 | *GRIN* mutations identified in the SNUH cohort patients**

Patient <sup>a</sup>	Variant information, domain <sup>b</sup>	Inheritance	ClinVar reported (P/LP)	Allele frequency	ACMG criteria	CADD score	Alpha missense <sup>c</sup>
<b><i>GRIN1</i> (NM_007327)</b>							
SNUH 1	c.1922T>A (p.Met641Lys), M3	de novo	N	NA	P	33	LP
SNUH 2	c.2443G>C (p.Gly815Arg), M4	de novo	Y	NA	P	36	LP
SNUH 3	c.1643G>A (p.Arg548Gln), Linker(S1-M1)	de novo	Y	NA	LP	34	LB
SNUH 4	c.1924A>T (p.Ile642Phe), M3	de novo	N	NA	P	32	LP
SNUH 5	c.2196C>G (p.Asp732Glu), S2	de novo	Y	NA	LP	24.3	LP
SNUH 6	c.1955C>T (p.Ala652Val), M3	de novo	Y	NA	P	33	LP
SNUH 7	c.1561_1563del (p.Asn521del), S1	de novo	N	NA	LP	NA	NA
SNUH 8	c.1600A>C (p.Lys534Gln), S1	de novo	N	NA	LP	29.9	LP
<b><i>GRIN2A</i> (NM_001134407)</b>							
SNUH 9	c.2246C>T (p.Thr749Ile), S2	de novo	N	NA	LP	30	LP
SNUH 10	c.1486A>G (p.Met496Val), S1	de novo	N	NA	LP	26.7	LP
SNUH 11	c.1553G>A (p.Arg518His), S1	unknown	Y	6.22e-7	P	34	LP
SNUH 12	c.2071G>A (p.Glu691Lys), S2	de novo	N	NA	LP	31	LP
<b><i>GRIN2B</i> (NM_000834)</b>							
SNUH 13	c.2459G>C (p.Gly820Ala), M4	de novo	Y	NA	P	28.4	LP
SNUH 15	c.2539C>T (p.Arg847Ter), CTD	unknown	Y	NA	P	43	NA
SNUH 17	c.2065G>A, (p.Gly689Ser), S2	unknown	Y	NA	P	33	LP
SNUH 19	c.2459G>C (p.Gly820Ala), M4	de novo	Y	NA	P	28.4	LP
SNUH 20	c.1883C>A (p.Ser628Tyr), Linker(M2-M3)	unknown	N	NA	P	32	LP
SNUH 21	c.2072C>T (p.Thr691Ile), S2	de novo	N	NA	P	32	LP
SNUH 22	c.2078G>C (p.Arg693Thr), S2	de novo	Y	NA	LP	28.8	LP
SNUH 23	c.2503_2511del (p.Thr835_Ile837del), M4	de novo	N	NA	LP	NA	NA
SNUH 24	c.1382G>A (p.Cys461Tyr), S1	de novo	Y	NA	P	32	LP
SNUH 25	c.2084T>C (p.Ile695Thr), S2	unknown	Y	NA	LP	33	LP
SNUH 26	c.2389C>T (p.Leu797Phe), S2	de novo	N	NA	LP	32	LP
SNUH 27	c.2539C>T (p.Arg847Ter), CTD	unknown	Y	NA	P	43	NA
SNUH 28	c.1556G>A (p.Arg519Gln), S1	de novo	Y	NA	P	33	LP
SNUH 29 <sup>d</sup>	c.2287G>A (p.Gly763Ser), S2	de novo	N	NA	LP	32	LP
SNUH 30 <sup>d</sup>	c.2287G>A (p.Gly763Ser), S2	de novo	N	NA	LP	32	LP
<b><i>GRIN2D</i> (NM_000836)</b>							
SNUH 31 <sup>e</sup>	c.2530A>C (p.Asn844His), M4	de novo	N	NA	LP	28.4	LP

ACMG American College of Medical Genetics, CADD Combined Annotation Dependent Depletion, CTD intracellular carboxy-terminal domains, P pathogenic, LP likely pathogenic, NA not available.

<sup>a</sup>SNUH 14, SNUH 16, and SNUH 18 confirmed *GRIN2B* deletion through chromosomal microarray.

<sup>b</sup>Domain was classified into amino-terminal domain, ligand-binding domain (S1 and S2), transmembrane domain (M1, M2, M3, and M4 helices), and intracellular carboxy-terminal domain (CTD).

<sup>c</sup>The cut-off values for pathogenic and benign are 0.560 and 0.340, respectively.

<sup>d</sup>Monozygotic twins sharing the same variant (*GRIN2B* c.2287G>A, p.Gly763Ser).

<sup>e</sup>Another de novo variant in *cis* with this variant was confirmed by Sanger sequencing (*GRIN2D* c.2489A>G, p.Asn830Ser).

based on their localization within the NMDA receptor, 15 variants (six in S1 and nine in S2) were located in the LBD, whereas seven variants (three in M3 and four in M4) were found in the TMD. One mutation was identified in each of the following regions: CTD, M2-M3 linker, and S1-M1 linker.

### Clinical characteristics of the SNUH cohort patients

The neurological phenotypes of patients are summarized in Table 2. Except for three patients (SNUH 1, SNUH 10, and SNUH 12) who presented with a chief complaint of seizures, the majority of patients visited the pediatric neurology clinic for GDD. Eighteen patients (58.1%) visited the pediatric neurology clinic before 12 months of age, and eight patients (25.8%) exhibited clinical seizures. The median observation period was 3 years (interquartile range [IQR]: 1.5–6.5 years). GDD was severe or profound, with 18 patients (58.1%) unable to walk independently and 23 (74.2%) unable to speak meaningful words. Additionally, nine patients (29.0%) had microcephaly (head circumference at age <3%), whereas one had macrocephaly (head circumference at age >97%). Eight patients had abnormal brain magnetic resonance imaging (MRI) findings, including one patient with polymicrogyria and two patients with delayed myelination. Lastly, one patient showed hypothyroidism (SNUH 10).

Eight patients in the SNUH cohort experienced clinical seizures, and their phenotypes are summarized in Table 3. The median age of seizure onset was 14 months (IQR: 9–31 months). Seizure types and electroencephalogram (EEG) findings varied among patients. Three patients achieved seizure freedom, with only one patient successfully tapering off antiseizure medication (ASM). Notably, four patients had abnormal EEG findings without clinical seizures. The most frequently prescribed initial ASM was valproic acid. However, drug-resistant epilepsy was common, with persistent epileptiform discharges observed in most patients during the last follow-up EEG. Responsive therapies included vigabatrin, valproic acid, oxcarbazepine, and the ketogenic diet.

Representative cases of *GRIN*-related NDDs are presented in Fig. 1. Figure 1a shows a patient who visited our clinic with a chief complaint of GDD, along with seizures and microcephaly. Initial brain MRI revealed delayed myelination, whereas follow-up imaging revealed diffuse brain atrophy. Trio whole-exome sequencing (WES) identified that the patient had a de novo missense mutation in the *GRIN1* gene (c.2443G>C) located within the M4 helix of the TMD. The patient expired with an unknown etiology at the age of 2 years and 11 months of age. Figure 1b shows monozygotic twins with the chief complaint of GDD. Notably, both patients presented very similar MRI findings, including nodular T2 hyperintensities in the brainstem (SNUH 29 and SNUH 30) and cerebellum (SNUH 30). They both presented with profound GDD with an inability to speak meaningful words and walk independently.

### Association between neurologic features and *GRIN* variant subtypes

The most prominent neurological phenotype was profound GDD (239 out of 349, 68.5%), with the highest prevalence in *GRIN1* (98 out of 123, 79.7%), followed by *GRIN2D* (14 out of 20, 70.0%) and *GRIN2B* (96 out of 138, 69.6%). Seizure prevalence varied by gene type and was the highest in patients with *GRIN2D* (20 out of 20, 100%) and *GRIN2A* (56 out of 68, 82.4%) variants, followed by those with *GRIN1* (71 out of 123, 57.7%) and *GRIN2B* (49 out of 138, 35.5%) variants (Fig. 2a and Supplementary Table 1). The neurological phenotypes of *GRIN* missense and in-frame variants are shown in Supplementary Fig. 1. The prevalence of neurological phenotypes was comparable across all *GRIN* gene types when limited to missense and in-frame variants. For instance, the prevalence of profound GDD in *GRIN2A* variants was the lowest at 45.6%, but increased to 60.4% when limited to missense and in-frame variants, making neurological phenotype prevalence comparable across *GRIN* gene types. Additionally, the prevalence of neurological phenotypes such as profound GDD (74.3% vs. 30.4%,  $p < 0.001$ ), movement disorder (MD) (69.0% vs. 41.4%,  $p < 0.01$ ), and malformation of cortical development (MCD) (21.4% vs. 0%,  $p < 0.01$ ) was significantly higher in patients with missense or in-frame variants than

in those with PTVs (Fig. 2b). The above analyses were conducted using only variants classified as pathogenic or likely pathogenic.

The distribution and characteristics of *GRIN* variants are summarized in Fig. 3. Among the 505 *GRIN* variants pooled from the ClinVar and SNUH cohorts, *GRIN2A* variants were the most frequent (211/505, 41.8%), followed by *GRIN2B* (199/505, 39.4%) (Fig. 3a). PTVs were most prevalent in patients with *GRIN2A* (99/214, 46.3%), followed by those with *GRIN2B* (56/196, 28.6%). In contrast, patients with *GRIN1* variants exhibited a lower prevalence of PTVs (7.5%), whereas no PTVs were reported among those with *GRIN2D* variants (Fig. 3b). Mapping of the missense and in-frame variant loci revealed clustering within regions encoding the M3 and M4 helices of the TMD (Fig. 3c and Supplementary Fig. 2).

Figure 4 shows the phenotypic profiles of the *GRIN* Portal and SNUH cohorts (Supplementary Table 2). We examined 349 patients with *GRIN*-related NDDs, including 123 with *GRIN1* variants, 68 with *GRIN2A* variants, 138 with *GRIN2B* variants, and 20 with *GRIN2D* variants. Patients with missense or in-frame variants in the M3–M4 helices of the TMD had the highest prevalence of various neurological phenotypes, except for those with ASD (Fig. 4a). Patients with M3 helix variants had the highest risk of profound GDD (adjusted odds ratio [aOR]: 8.48, 95% confidence interval [CI]: 2.79–25.76), ataxia (aOR: 5.33, 95% CI: 1.34–21.12), and cortical visual impairment (CVI) (aOR: 3.89; 95% CI: 1.60–9.48). Patients with M4 helix variants had the highest risk of MD (aOR: 11.40, 95% CI: 2.58–50.37) (Fig. 4b).

### Discussion

This study investigated an in-depth analysis of the clinical phenotypes associated with *GRIN*-related NDDs in the SNUH and *GRIN* Portal cohorts. The most consistent finding across the cohort was profound GDD. The neurological manifestations were diverse, including ASD and MD, with genotype-specific patterns and significant associations with variant localization within the NMDA receptor.

Profound GDD was the most common phenotype observed, which is consistent with the findings of previous studies<sup>9,10</sup>. However, earlier studies often focused solely on investigating patients exhibiting intellectual disability and speech problems, without considering the severity of GDD. Our findings highlight that most patients present severe developmental challenges from infancy, with the majority failing to achieve basic milestones, such as independent walking and speaking simple words by 12 months of age. Notably, some patients experienced developmental regression, further underscoring the profound impact of *GRIN* variants on neurodevelopment. Furthermore, most children exhibited severe cognitive impairment that could not carry out full-scale intelligence quotient testing. Additionally, brain MRI imaging, performed as part of the diagnostic process, did not reveal consistent structural abnormalities.

In addition to profound GDD, phenotypic manifestations varied by gene. Seizures were more prominent in patients with *GRIN2A* and *GRIN2D* variants, whereas MD was more prominent in patients with *GRIN1* variants. Sapuppo et al.<sup>11</sup> demonstrated that *GRIN2A* variants were linked to Landau-Kleffner syndrome, whereas *GRIN2B* variants were linked to West syndrome. However, we were unable to identify any specific epilepsy patterns in the SNUH cohort. This study highlights the neurological phenotypic overlap among pediatric patients with *GRIN* variants and suggests genotype-specific differences in detailed phenotypes. Notably, the differences in variant type distribution, such as the PTVs primarily observed in patients with *GRIN2A* and *GRIN2B* variants, may have contributed to the clinical differences between the genes (Fig. 2 and Supplementary Fig. 1).

Previous studies have shown that patients with *GRIN* PTVs have a significantly lower risk of severe intellectual disability compared to those with missense variants<sup>3,12</sup>. Notably, Santos-Gomez et al. investigated the clinical characteristics of patients with *GRIN2A* and *GRIN2B* PTVs, reporting that *GRIN2A* variants were associated with seizures, whereas *GRIN2B* variants were linked to ASD<sup>12</sup>. In line with our findings, patients with missense or in-frame variants exhibited a broader range of neurological phenotypes—including not only GDD and seizures, but also MD and MCD

**Table 2 | Phenotypic characteristics of patients with GRIN mutations of the SNUH cohort**

Patient	Gene	Age at onset	Sex/age (y) <sup>a</sup>	Latest developmental status	Developmental milestone	HC <sup>b</sup>	Movement/behavior	Brain MRI	Seizure	Other features
SNUH 1	GRIN1	<1 m	F/7.5	Head control, cannot roll over, no meaningful words	NA	WNL	Myoclonus, irritability, dystonia	Chiari I malformation	Y	Increased CSF-to-plasma glycine ratio, tracheostomy, rectal prolapse,
SNUH 2	GRIN1	11 m	M/2.5	Sit with support, no meaningful words	Head control unavailable, poor eye contact at 24 m	▼	Myoclonus	Delayed myelination, diffuse brain atrophy	Y	Nystagmus, increased CSF-to-plasma glycine ratio, sudden cardiac arrest (2 y 11 m)
SNUH 3	GRIN1	7 m	M/6	Walk with holding, eye contact, visual tracking	Roll over at 6 m, sit alone, babbling only at 18 m	▼	Rett-like behavior <sup>c</sup> , sleep disturbance	WNL	N	Strabismus
SNUH 4	GRIN1	5 m	M/9	Roll over, cannot recognize parents	Social smile, poor head control at 4 y 6 m	▼	Jitteriness, hyperkinetic movement, facial dyskinesia	Delayed myelination	N	
SNUH 5	GRIN1	4 m	F/4.5	Walk upstairs with support, say 6–7 words	Head control at 4 m, roll over at 6 m, crawl and babbling at 18 m	WNL	NA	WNL	N	Preterm birth (GA 33 + 2 weeks, 1.9 kg)
SNUH 6	GRIN1	6 m	M/3.5	Head control, rolling, no meaningful words	Cannot head control and roll over at 20 m	▼	NA	WNL	N	
SNUH 7	GRIN1	7 m	M/6	Run alone, moderate ID	Walk alone at 24 m	NA	ASD	WNL	Y	FSIQ 42
SNUH 8	GRIN1	1 y	F/2	Walk a few steps, only babbling	Sit alone and babbling at 1 y	WNL	Normal	WNL	N	Preterm birth (GA 33 + 6 weeks, 2.0 kg)
SNUH 9	GRIN2A	1 y	F/15.5	Walk alone, no meaningful words (regression during infancy)	Stand with holding, recognize parents at 6 y	NA	Rett-like behavior <sup>c</sup> , hyperkinetic movement	WNL	N	Strabismus, polydactyly
SNUH 10	GRIN2A	3 m	F/2	Head control, eye contact, cannot sit alone	Incomplete head control at 6 m	▼	Dystonia, dyskinesia	WNL	N	Hypothyroidism, Leber congenital amaurosis
SNUH 11	GRIN2A	1 y 1 m	M/2	Stand with holding, only babbling	NA	WNL	Myoclonus	WNL	Y	
SNUH 12	GRIN2A	4 y 10 m	M/8	GDD	NA	NA	NA	WNL	Y	
SNUH 13	GRIN2B	8 m	F/16	Sit with support, no meaningful words	Roll over at 6 y	▼	Rett-like behavior <sup>c</sup> , ASD	WNL	N	
SNUH 14	GRIN2B	1 y 7 m	F/3.5	10–20 words, simple obey command	Head control at 3 m, stand alone, babbling at 20 m	NA	Normal	WNL	N	FSIQ 76
SNUH 15	GRIN2B	1 y 3 m	M/3	Running, say 2–3 words	Roll over at 6 m, walk alone at 2 y	WNL	Normal	WNL	N	
SNUH 16	GRIN2B	1 y 2 m	M/5.5	2-word sentence, running	Walk alone, say 2 words at 2 y	WNL	ASD, ADHD	WNL	Y	FSIQ 60
SNUH 17	GRIN2B	5 m	F/1.5	Roll over, social smile	Cannot control head at 5 m	WNL	NA	Mild brain atrophy	N	
SNUH 18	GRIN2B	8 m	F/6	Can recite some English letters and numbers	Stand with support, 2–3 words at 2 y	WNL	NA	Arachnoid cyst	N	FSIQ 47, intestinal duplication
SNUH 19	GRIN2B	2 m	F/7	Cannot walk alone, sit alone, developmental regression	Roll over, babbling at 4.5 y	▼	Rett-like behavior <sup>c</sup>	WNL	N	Cortical visual impairment
SNUH 20	GRIN2B	6 m	M/4.5	Sit alone, do not see when called	Roll over at 1 y, babbling at 1.5 y	WNL	NA	WNL	N	
SNUH 21	GRIN2B	11 m	M/3	Sit alone, see when called, recognize parents	Babbling, eye contact, cannot control head at 10 m	WNL	Normal	WNL	N	
SNUH 22	GRIN2B	10 m	F/10.5	Cannot roll over, sit alone, babbling only	Head control at 26 m, see when called at 39 m	▼	NA	Cortical thickening, polymicrogyria	Y	Facial dysmorphism (downward slanted palpebral fissure)
SNUH 23	GRIN2B	6 m	F/3.5	Walk alone, no meaningful words	Stand alone, say 2 words at 2 y	▲	NA	WNL	N	
SNUH 24	GRIN2B	3 y 3 m	M/30	Severe ID	Roll over at 9 m, walk with support at 2 y	WNL	NA	WNL	N	FSIQ 37

**Table 2 (continued) | Phenotypic characteristics of patients with GRIN mutations of the SNUH cohort**

Patient	Gene	Age at onset	Sex/age (y) <sup>a</sup>	Latest developmental status	Developmental milestone	HC <sup>b</sup>	Movement/behavior	Brain MRI	Seizure	Other features
SNUH 25	GRIN2B	1 y	M/8.5	Autistic behavior, severe GDD	Stand with holding at 2 y, 2-word sentence at 4 y	WNL	ASD	WNL	N	FSIQ 44
SNUH 26	GRIN2B	2 y	F/6.5	2-word sentence, simple obey command	Walk alone at 2 y	WNL	ASD	NA	N	FSIQ 47
SNUH 27	GRIN2B	2 y 6 m	M/4	Running, a few words	Walk alone at 19 m, first word at 2 y	▼	ASD	NA	N	FSIQ 47, facial dysmorphism (cupped ear, micrognathia)
SNUH 28	GRIN2B	1 y 9 m	M/2	A few words, walk alone	Stand alone, meaningful words at 21 m,	WNL	NA	NA	N	
SNUH 29 <sup>d</sup>	GRIN2B	10 m	F/2	Sit with support, imitative action, babbling	Head control at 7 m	WNL	NA	T2 hyperintensities from midbrain to medulla	N	
SNUH 30 <sup>d</sup>	GRIN2B	10 m	F/2	Roll over, no meaningful words	Head control at 7 m	WNL	NA	Nodular T2 hyperintensities at brainstem and cerebellum	N	
SNUH 31	GRIN2D	1 y 1 m	F/3	Walk alone, babbling, simple obey command	Stand with support, cannot perform a pincer grasp at 15 m	WNL	NA	WNL	Y	

y year, HC head circumference, MRI magnetic resonance imaging, F female, CSF cerebrospinal fluid, M male, m month, GA gestational age, ID intellectual disability, ASD autism spectrum disorder, GDD global developmental delay, FSIQ full-scale intelligence quotient, ADHD attention-deficit hyperactivity disorder, WNL within normal limit, NA not available.

<sup>a</sup>Age at last review with pediatric neurologists.

<sup>b</sup>▲ represents macrocephaly (head circumference for age >97%) and ▼ represents microcephaly (head circumference for age <3%).

<sup>c</sup>Includes stereotypical features, such as habitual or uncontrollable hand stereotypy, and bruxism.

<sup>d</sup>Monozygotic twins sharing the same variant (GRIN2B c.2287G>A, p.Gly763Ser).

—compared to those with PTVs<sup>3,12</sup>. By integrating genotypic and phenotypic information from 349 patients with *GRIN* variants (including 46 with PTVs), our study expands the current understanding of *GRIN*-related NDD phenotypes according to variant type.

We analyzed the detailed responses to ASM in the SNUH cohort. Our results suggest that medications, such as vigabatrin and valproic acid, may be effective options for managing seizures in *GRIN*-related NDDs. However, due to the lack of ASM response data in the GRIN Portal, a more detailed analysis based on variant subtypes was not available. To enable personalized medicine and tailor therapeutic options for *GRIN*-related NDDs, a comprehensive database containing detailed clinical information must be developed.

The differences in the prevalence of neurological phenotypes among *GRIN* gene subtypes may be attributed to the distinct spatiotemporal expression patterns of the *GRIN* gene<sup>3</sup>. GluN2A, encoded by *GRIN2A*, is initially expressed postnatally and becomes abundant during brain maturation. On the other hand, GluN2B, encoded by *GRIN2B*, is widely expressed during embryogenesis and remains highly prominent in the forebrain during early development. Nevertheless, as shown in Fig. 2a and Supplementary Fig. 1, gene-specific characteristics were not clearly defined, and the prevalence of each phenotype appeared more comparable when restricted to missense and in-frame variants.

As depicted in Fig. 3c, pathogenic and likely pathogenic variants tended to be located adjacent to the TMD domain helices M3 and M4, particularly in *GRIN1* and *GRIN2D*<sup>3</sup>. Myers et al.<sup>7</sup> showed that this critical region is under greater selection pressure and is highly intolerant to genetic variations. Korinek et al. demonstrated that missense variants located adjacent to the ABD and TMD tend to affect glutamate or glycine affinity<sup>13</sup>. These changes in affinity may contribute to either GoF or loss-of-function (LoF) of NMDA receptors, potentially leading to various neurological symptoms. We observed that the prevalence of profound GDD did not differ significantly by *GRIN* gene subtype but varied considerably by missense or in-frame variant domains. Notably, the severity and diversity of neurological phenotypes were more pronounced in missense or in-frame variants within the M3 and M4 helices than in the PTVs. This finding is in line with that of a recent study by Xu et al.<sup>8</sup>, which predicted that most variants within the M3 helix would be dysfunctional and pathological. Among the 48 variants located in the M3 domain, functional analysis revealed that 28 exhibited GoF, whereas only nine showed LoF, collectively suggesting that these variants enhanced channel gating activities. The M3 helix, which is directly linked to the ABD domain, plays a pivotal role in controlling channel opening and closing<sup>8,14</sup>. Although studies on the role of the M4 domain in channel function are currently limited to receptor modulation, our findings emphasize the clinical significance of the M4 domain in the neurological phenotypes of *GRIN*-related NDDs.

Our study, which included a large cohort of 349 patients, supports previous findings on the clinical relevance of missense variants in the M3 and M4 helices<sup>4,8</sup>. Patients with missense variants in affected domains exhibited a higher incidence of neurological phenotypes, such as profound GDD, MD, and ataxia, than those with variants in other domains. Additionally, we observed distinct phenotypic differences between the two helices, with the risk of seizures and ataxia being more prominent in the M3 helix. Although the underlying mechanisms remain unclear, our findings highlight the importance of domain-level interpretation, which may support phenotype prediction and the implementation of precision medicine in *GRIN*-related NDDs.

Based on the characteristics of the *GRIN* gene, previous studies have explored the use of NMDA receptor blockers (e.g., ketamine and memantine) in patients with *GRIN*-related NDD<sup>15,16</sup>. Nevertheless, as both GoF and LoF variants of *GRIN2A* result in prolonged NMDAR-mediated synaptic current decay, their clinical applications warrant further investigation. Additionally, with regard to the functional differences among the domains, previous studies have suggested that the M3 helix increases the potency of glutamate and glycine, whereas the M4 helix interacts with the

**Table 3 | Seizure characteristics of the SNUH cohort patients**

Patient	Variant information <sup>a</sup>	Initial features			Latest features			EEG findings	Seizure frequency	EEG findings
		Onset	Seizure type	Initial ASM	Responsive ASM	Age	Seizure type			
SNUH 1	<i>GRIN1</i> , p.Met641Lys (M3)	<1 m	IS	B6, VGB, PD		7.5 y	TS, GTC	OXC, B6	OXC	DCD
SNUH 2	<i>GRIN1</i> , p.Gly815Arg (M4)	11 m	FS	VPA	VPA	2.5 y	TS	VPA, CLB, VGB	VGB	1/week
SNUH 7	<i>GRIN1</i> , p.Asn521del (S1)	7 m	IS	VGB, B6	VGB	6 y	Seizure free			Focal spikes (F)
SNUH 11	<i>GRIN2A</i> , p.Arg518His (S1)	1 y 1 m	FS, MyS	VPA		2 y	FS, MyS	KD		Unknown
SNUH 12	<i>GRIN2A</i> , p.Glu691Lys (S2)	4 y 11 m	CS	VPA		8 y	FS with impaired awareness	VPA, KD	KD	<1/month
SNUH 16	<i>GRIN2B</i> (chr12:13,866,171-14,123,390 deletion)	1 y 2 m	TS	LEV, PB, TPM		5.5 y	Seizure free	CLB, OXC, VPA	OXC	Normal
SNUH 22	<i>GRIN2B</i> , p.Arg693Thr (S2)	3 y 1 m	GTC	VPA	VPA	10.5 y	Seizure free	VPA, CNZ		Generalized spike bursts
SNUH 31	<i>GRIN2D</i> , p.Asn844His (M4)	2 y	MyS	VPA		3 y	MyS, TS	VPA, CLB, VGB	VGB	A few times/day

ASM antiseizure medication, EEG electroencephalogram, m month, IS infantile spasms, B6 pyridoxine, VGB vigabatrin, PD prednisolone, B-S background suppression, y year, TS tonic seizure, GTC generalized tonic-clonic, OXC oxcarbazepine, DCD diffuse cerebral dysfunction, FS focal seizure, VPA valproate, O occipital, CLB clobazam, Hyps hypsarrhythmia, F frontal, MyS myoclonic seizure, LEV levetiracetam, PB phenobarbital, TPM topiramate, C central, CNZ clobazepam.

<sup>a</sup>Variant information (domain or genomic information). M3 or M4 domain stands for the transmembrane domain of the *GRIN* gene. S1 or S2 domain stands for the ligand-binding domain of the *GRIN* gene. SNUH 16 confirmed 257 kb deletion through chromosomal microarray.

M1 and M3 helices to modulate receptor activity. However, further research is required to better understand these mechanisms<sup>1,8,14</sup>.

As demonstrated in representative cases, patients with *GRIN*-related NDDs typically present with profound GDD during infancy, which is characterized by limited developmental progress. Previous studies have reported that the MRI findings of patients with *GRIN*-related NDDs include cortical atrophy and increased white matter signal intensity in the periventricular white matter<sup>17,18</sup>. To our knowledge, the MRI findings shown in Fig. 1b have not been previously reported. We hypothesize that these features may be attributed to a genetic etiology and could be distinctive characteristics of *GRIN* variants. Notably, identical findings were observed in the monozygotic twins, further supporting the genetic basis of these manifestations.

The strength of our study lies in the detailed phenotyping of patients with *GRIN* variants from the SNUH cohort, including 13 with previously unreported variants. Our findings expand our understanding of the phenotypic spectrum and phenotype-genotype correlations in *GRIN*-related NDDs. To our knowledge, this study is the first to present a series of cases involving pediatric patients with *GRIN* variants and neurological phenotypes in an Asian population. Our study has some limitations, including the lack of functional validation and the small sample size, which limit the generalizability of the findings to the full spectrum of *GRIN*-related NDDs. However, our detailed phenotyping, including ASM responses and developmental milestones, provides clinically relevant insights for the personalized management of patients with *GRIN*-related NDDs.

This study included a total of 349 patients by combining the SNUH cohort and the *GRIN* Portal dataset. Although our study represents one of the largest datasets of *GRIN*-related NDD, there remains considerable potential to incorporate a much larger number of patients and variants. As observed in the SNUH cohort, where more than 50% of the variants were novel, a substantial number of pathogenic variants likely remain unreported. Furthermore, a considerable proportion of pathogenic or likely pathogenic variants previously submitted to ClinVar have not yet been incorporated into the *GRIN* Portal. Even among those included in the *GRIN* Portal, over 200 variants were excluded due to insufficient clinical information. In particular, the rate of missing data for ASD, MD, ataxia, and CVI was notably higher than that of seizures and GDD. These findings highlight the need to develop a more comprehensive database that encompasses a broader spectrum of genotypes and phenotypes. Further research utilizing large-scale datasets is warranted to better elucidate genotype-phenotype correlations in *GRIN*-related NDDs.

In conclusion, this study presents the genetic and clinical presentations of *GRIN*-related NDDs. *GRIN* variants are associated with profound GDD accompanied by various neurological manifestations. Patients with pathogenic missense or in-frame variants in the M3 and M4 helices of the TMD exhibited significantly distinctive phenotypes. The evaluation of the specific variant domains of *GRIN* mutations provides valuable insights into the clinical characteristics.

## Methods

### Study participants

We enrolled 31 patients with genetically confirmed *GRIN* mutations (8 with *GRIN1*, 4 with *GRIN2A*, 18 with *GRIN2B*, and 1 with *GRIN2D*). All patients were evaluated at the Pediatric Neurology Clinic of SNUH. The study was performed in accordance with the ethical standards of the Declaration of Helsinki and approved by the Institutional Review Board of SNUH (H-2408-063-1559). The requirement for informed consent was waived, as the research involved minimal risk and used de-identified retrospective data. All participants were unrelated, except for a pair of monozygotic twins who shared the same *GRIN2B* pathogenic variant (SNUH 29 and SNUH 30).

*GRIN* variants were distributed across the *GRIN1*, *GRIN2A*, *GRIN2B*, and *GRIN2D* genes. The clinical information of the SNUH cohort was retrospectively reviewed using electronic medical records, including neurological phenotypes such as GDD, MD, and ASD. Neurodevelopmental

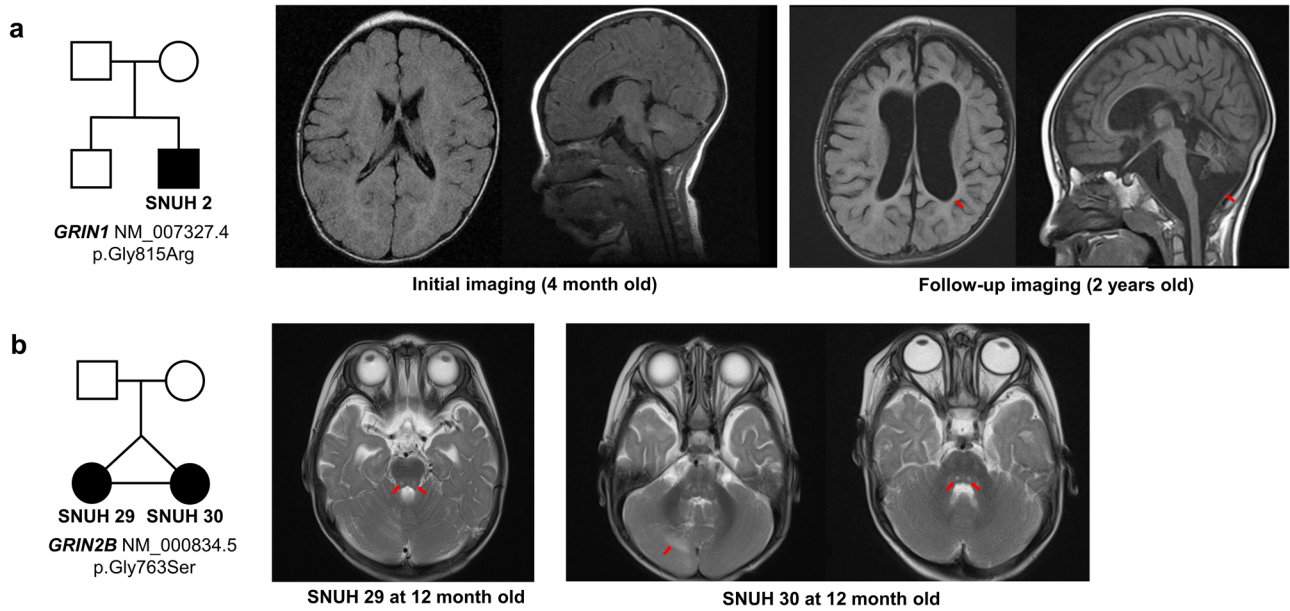
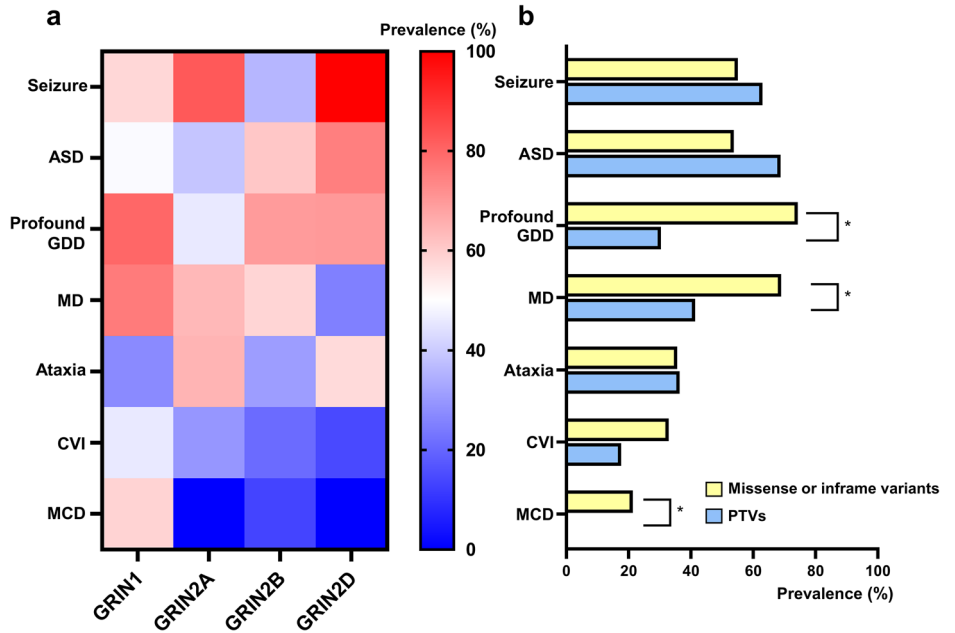


**Fig. 1 | Representative cases of GRIN-related neurodevelopmental disorders.** **a** Clinical information of SNUH 2, who presented with a chief complaint of profound GDD at four months of age. The patient was found to have a de novo *GRIN1* missense variant located in the M4 helix of TMD (c.2443G>C, p.Gly815Arg). An initial brain MRI acquired at four months of age showed delayed myelination, while follow-up imaging at two years old showed diffuse brain atrophy. **b** Clinical

information of SNUH 29 and SNUH 30, monozygotic twins presenting with a chief complaint of profound GDD. Quartet whole-exome sequencing analysis identified a de novo *GRIN2B* missense variant (c.2287G>A, p.Gly763Ser) in both twins. Brain MRI acquired at 12 months old revealed nodular T2 hyperintensities in the brainstem (SNUH 29, SNUH 30) and cerebellum (SNUH 30). TMD transmembrane domain, GDD global developmental delay, MRI magnetic resonance imaging.

**Fig. 2 | Prevalence of neurological phenotypes among pooled variants (including data from the GRIN Portal and the SNUH cohort), stratified by gene type and variant type.** Prevalence of neurological phenotypes stratified by **a** gene type and **b** variant type. \* $p < 0.05$ . ASD autism spectrum disorder, GDD global developmental delay, MD movement disorder, CVI cortical visual impairment, MCD malformation of cortical development, PTV protein-truncating variant.



status was evaluated at the initial and most recent visits. Additional clinical data included EEG and brain MRI results. The detailed seizure characteristics of eight patients with epilepsy, including semiology and ASM usage, were also collected.

**Genetic diagnosis**

The *GRIN* variants in the SNUH cohort were identified using NGS. Of them, 23 patients were analyzed by trio WES, five by singleton WES, and three by chromosomal microarray (CMA). WES was performed at our institution using the Illumina technology. The

generated reads were aligned to the human reference genome (hg38) and processed according to the Genome Analysis Toolkit best practice guidelines<sup>19</sup>. Then, the variants were annotated using the ANNOVAR program, with a focus on rare protein-altering variants with a population allele frequency of <0.001% based on the Genome Aggregation Database (gnomAD)<sup>20,21</sup>. The Human Gene Mutation Database and ClinVar database were searched for previously reported variants<sup>22,23</sup>. Variants were interpreted using the criteria established by the American College of Medical Genetics and Genomics/Association for Molecular Pathology (ACMG/AMP) criteria<sup>24</sup>. All



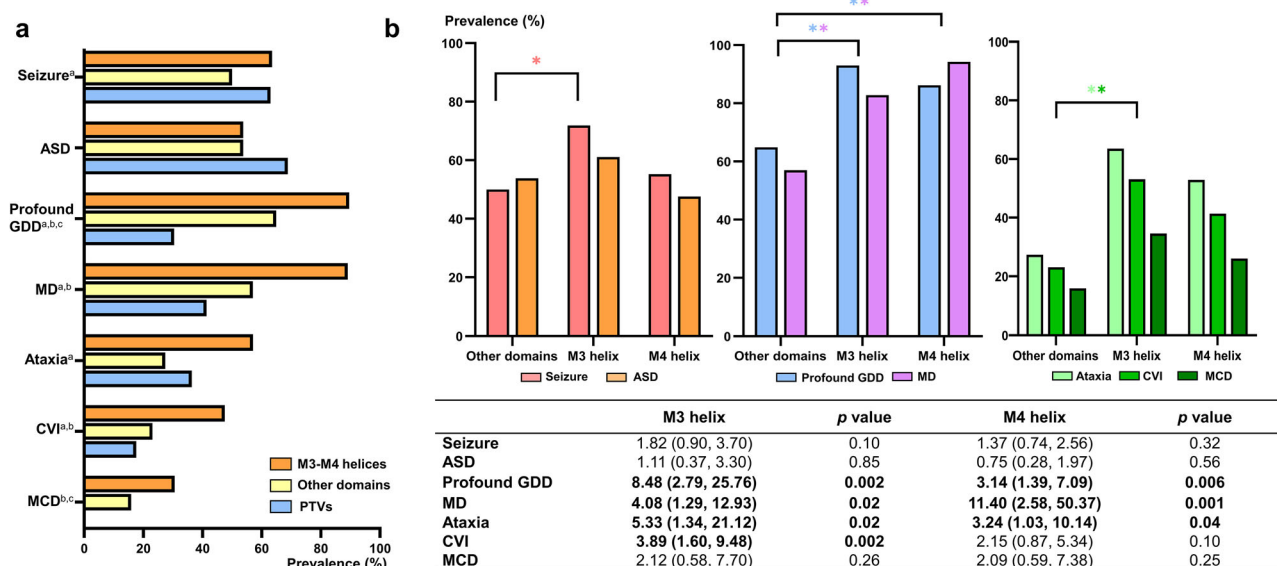


**Fig. 4 | Prevalence and risk of neurological phenotypes among pooled variants (including data from the GRIN Portal and the SNUH cohort), stratified by variant domains. a** Comparisons among M3–M4 helices, other domains, and PTVs. **b** Prevalence and risk of neurological phenotypes across missense or in-frame variant domains (other domains, M3 helix, and M4 helix of each *GRIN* gene) presented as odds ratios with 95% confidence intervals, adjusted for *GRIN* gene subtypes.

<sup>a</sup> $p < 0.05$  for comparisons between missense or in-frame variants in M3–M4 helices and those in other domains. <sup>b</sup> $p < 0.05$  for comparisons between in-frame variants in the M3–M4 helices and PTVs. <sup>c</sup> $p < 0.05$  for comparisons between missense or in-frame variants in other domains and PTVs. \* $p < 0.05$ . GDD global developmental delay, ASD autism spectrum disorder, MD movement disorder, CVI cortical visual impairment, MCD malformation of cortical development.

Fisher’s exact test applied for post-hoc analysis. Logistic regression analysis was conducted to assess the association between neurological phenotypes and variant domains, with a focus on variants located in the M3 and M4 helices of the TMD.

The associations were expressed as aOR and 95% CIs, adjusted for gene subtype. All analyses were performed using R (version 4.0.4; R Foundation for Statistical Computing) and GraphPad Prism version 8.0 (GraphPad Software), with a significance level of  $p < 0.05$  considered significant. *GRIN* variants from the SNUH cohort and ClinVar databases were visualized using the PeCan protein viewer<sup>27</sup>. The identified variants were annotated in accordance with the Human Genome Variation Society guidelines<sup>28</sup>.

### Data availability

The datasets analyzed during the current study are available from the corresponding author upon reasonable request.

Received: 27 January 2025; Accepted: 2 May 2025;

Published online: 15 May 2025

### References

- Langer, K., Müller-Längle, A., Wempe, J. & Laube, B. Analysis of M4 transmembrane segments in NMDA receptor function: a negative allosteric modulatory site at the GluN1 M4 is determining the efficiency of neurosteroid modulation. *Front. Pharmacol.* **12**, 769046 (2021).
- Paoletti, P., Bellone, C. & Zhou, Q. NMDA receptor subunit diversity: impact on receptor properties, synaptic plasticity and disease. *Nat. Rev. Neurosci.* **14**, 383–400 (2013).
- Platzer, K. et al. GRIN2B encephalopathy: novel findings on phenotype, variant clustering, functional consequences and treatment aspects. *J. Med. Genet.* **54**, 460–470 (2017).
- Strehlow, V. et al. GRIN2A-related disorders: genotype and functional consequence predict phenotype. *Brain* **142**, 80–92 (2019).
- XiangWei, W., Jiang, Y. & Yuan, H. De novo mutations and rare variants occurring in NMDA receptors. *Curr. Opin. Physiol.* **2**, 27–35 (2018).
- Lee, C.-H. et al. NMDA receptor structures reveal subunit arrangement and pore architecture. *Nature* **511**, 191–197 (2014).
- Myers, S. J. et al. Distinct roles of GRIN2A and GRIN2B variants in neurological conditions. *F1000Research* **8** (2019).
- Xu, Y. et al. De novo GRIN variants in M3 helix associated with neurological disorders control channel gating of NMDA receptor. *Cell. Mol. Life Sci.* **81**, 153 (2024).
- Benke, T. A. et al. Clinical and therapeutic significance of genetic variation in the GRIN gene family encoding NMDARs. *Neuropharmacology* **199**, 108805 (2021).
- García-Recio, A. et al. GRIN database: a unified and manually curated repertoire of GRIN variants. *Hum. Mutat.* **42**, 8–18 (2021).
- Sapuppo, A. et al. GRIN2A and GRIN2B and their related phenotypes. *J. Pediatr. Neurol.* **21**, 212–223 (2023).
- Santos-Gómez, A. et al. Disease-associated GRIN protein truncating variants trigger NMDA receptor loss-of-function. *Hum. Mol. Genet.* **29**, 3859–3871 (2020).
- Korinek, M. et al. Disease-associated variants in GRIN1, GRIN2A and GRIN2B genes: insights into NMDA receptor structure, function, and pathophysiology. *Physiol. Res.* **73**, S413 (2024).
- Li, J. et al. De novo GRIN variants in NMDA receptor M2 channel pore-forming loop are associated with neurological diseases. *Hum. Mutat.* **40**, 2393–2413 (2019).
- Eiler, I. et al. GRIN1-related epilepsy in a neonate with response to memantine and vigabatrin. *Ann. Child Neurol. Soc.* **2**, 299–302 (2024).
- Xu, Y. et al. Recurrent seizure-related GRIN1 variant: molecular mechanism and targeted therapy. *Ann. Clin. Transl. Neurol.* **8**, 1480–1494 (2021).
- Pironti, E. et al. Electroclinical history of a five-year-old girl with GRIN1-related early-onset epileptic encephalopathy: a video-case study. *Epileptic Disord.* **20**, 423–427 (2018).
- XiangWei, W. et al. Heterogeneous clinical and functional features of GRIN2D-related developmental and epileptic encephalopathy. *Brain* **142**, 3009–3027 (2019).
- McKenna, A. et al. The genome analysis toolkit: a MapReduce framework for analyzing next-generation DNA sequencing data. *Genome Res.* **20**, 1297–1303 (2010).

20. Wang, K., Li, M. & Hakonarson, H. ANNOVAR: functional annotation of genetic variants from high-throughput sequencing data. *Nucleic Acids Res.* **38**, e164 (2010).
  21. Karczewski, K. J. et al. The mutational constraint spectrum quantified from variation in 141,456 humans. *Nature* **581**, 434–443 (2020).
  22. Landrum, M. J. et al. ClinVar: improving access to variant interpretations and supporting evidence. *Nucleic Acids Res.* **46**, D1062–D1067 (2018).
  23. Stenson, P. D. et al. The Human Gene Mutation Database: towards a comprehensive repository of inherited mutation data for medical research, genetic diagnosis and next-generation sequencing studies. *Hum. Genet.* **136**, 665–677 (2017).
  24. Richards, S. et al. Standards and guidelines for the interpretation of sequence variants: a joint consensus recommendation of the American College of Medical Genetics and Genomics and the Association for Molecular Pathology. *Genet. Med.* **17**, 405–423 (2015).
  25. Lee, S. et al. TNNT1 myopathy with novel compound heterozygous mutations. *Neuromuscul. Disord.* **32**, 176–184 (2022).
  26. Consortium, U. UniProt: a worldwide hub of protein knowledge. *Nucleic Acids Res.* **47**, D506–D515 (2019).
  27. McLeod, C. et al. St. Jude Cloud: a pediatric cancer genomic data-sharing ecosystem. *Cancer Discov.* **11**, 1082–1099 (2021).
  28. Den Dunnen, J. T. et al. HGVS recommendations for the description of sequence variants: 2016 update. *Hum. Mutat.* **37**, 564–569 (2016).
- B.C.L., K.J.K., and S.L.; data curation: J.H.C., S.L.; writing – original draft preparation: J.H.C., S.L.; writing – review and editing: W.K., S.Y.K., B.C.L., K.J.K., and J.-H.C.; visualization: J.H.C., S.L.; supervision: W.K., S.Y.K., B.C.L., K.J.K.; funding acquisition: S.L., B.C.L., J.-H.C. The authors read and approved the final manuscript.

### Competing interests

The authors declare no competing interests.

### Additional information

**Supplementary information** The online version contains supplementary material available at <https://doi.org/10.1038/s41525-025-00499-z>.

**Correspondence** and requests for materials should be addressed to Seungbok Lee.

**Reprints and permissions information** is available at <http://www.nature.com/reprints>

**Publisher's note** Springer Nature remains neutral with regard to jurisdictional claims in published maps and institutional affiliations.

**Open Access** This article is licensed under a Creative Commons Attribution-NonCommercial-NoDerivatives 4.0 International License, which permits any non-commercial use, sharing, distribution and reproduction in any medium or format, as long as you give appropriate credit to the original author(s) and the source, provide a link to the Creative Commons licence, and indicate if you modified the licensed material. You do not have permission under this licence to share adapted material derived from this article or parts of it. The images or other third party material in this article are included in the article's Creative Commons licence, unless indicated otherwise in a credit line to the material. If material is not included in the article's Creative Commons licence and your intended use is not permitted by statutory regulation or exceeds the permitted use, you will need to obtain permission directly from the copyright holder. To view a copy of this licence, visit <http://creativecommons.org/licenses/by-nc-nd/4.0/>.

© The Author(s) 2025

### Acknowledgements

We sincerely acknowledge the GRIN Portal database (<https://grin-portal.broadinstitute.org/>) for systematically compiling and making available comprehensive genetic and clinical information on patients with *GRIN*-related neurodevelopmental disorders. This research was supported by a grant from the Korea Health Technology R&D Project through the Korea Health Industry Development Institute (KHIDI), funded by the Ministry of Health & Welfare, Republic of Korea (grant number: RS-2023-00265923), and by the SNUH Lee Kun-hee Child Cancer & Rare Disease Project, Republic of Korea (grant number: 22B-001-0100).

### Author contributions

Conceptualization: J.H.C., S.L., and J.-H.C.; methodology: J.M.K., H.-J.Y., and H.C.; investigation: J.H.C.; validation: S.L.; formal analysis: J.H.C., J.M.K., H.-J.Y., and H.C.; access and verification of the data: H.J.K., S.Y.K.,